

Electrochemical Behavior of Nickel Alloys and Stainless Steel in HNO₃ using Cyclic Voltammetry Technique

M. Abdallah^{1,2,*}, B.A.AL Jahdaly², M.M. Salem³, A. Fawzy,^{2,4} E.M. Mabrouk¹

1. Chemistry Department, Faculty of Science, Benha University, Benha, Egypt

2. Chemistry Department., Faculty of Applied Sciences, Umm Al-Qura University, Makkah, Saudi Arabia.

3. Chemistry Department, Faculty of Education in Zulfi, Majmaah University, Saudi Arabia

4. Chemistry Department, Faculty of Science, Assiut University, Assiut, Egypt

Received 01 Jan 2017,

Revised 29 Jan 2017,

Accepted 06 Feb 2017

Keywords

- ✓ Nickel;
- ✓ Inconel600;
- ✓ Incoloy800;
- ✓ 316 Stainless Steel;
- ✓ Cyclic Voltammetry

M. Abdallah

metwally555@yahoo.com

+966580369045

Abstract

The electrochemical behavior of nickel, Inconel600, Incoloy800 and 316 stainless steel in different concentrations of HNO₃ solutions was investigated using the cyclic voltammetry technique. . All the curves in the anodic cyclic voltammetry are characterized by an anodic dissolution peak (A) followed by a passive region (B), before oxygen evolution. On the other hand incoloy800 and 316 stainless steel show an additional dissolution peak (C) and trans passive region followed by oxygen evolution. In the cathodic branch of the CVS there is one cathodic peak in the case of Ni. Inconel600 and Incoloy800. On the other hand, there is an unexpected peak in case of 316 stainless steel. This peak appeared on the anodic branch. All the anodic and cathodic peaks are interpreted. The passivation of Ni was explained based on the formation of NiO. In the alloys the passive layer was mainly composed of Ni⁺², Fe⁺³ and Cr⁺³ in Inconel600, Incoloy800, and Mo⁺⁶ in case of 316 stainless steel. The role of Cr⁺³ and Mo⁺⁶ ions in the reinforcement of the passive film is explained.

1. Introduction

Nickel and its alloys are used in various industrial applications [1,2]. Nickel is widely used as an alloying element because it impacts strength, toughness and corrosion resistance [3,4]. In industrial processes the acidic solutions are commonly used in an acid bath in plating, electro winning and pickling process. High nickel alloys were used in heat exchanger and various elements of pressurized water reactors. The main application of stainless steel in petroleum and food processing equipment's. Nickel-base alloys and stainless steel offer excellent corrosion resistance to a wide range of corrosive media due to the formation of a stable passive film on the metal surface [5-7]. The stability of this passive film is damaged and pitting corrosion occurs when these alloys are polarized above some electrode potentials in environments containing certain aggressive ions such as chloride [8-9].

The potentiostatic current –potential curves of nickel in nitric acid solutions were classified into three categories according to the proportion of acid concentration [10]. At concentration, less than 8M the behavior is similar to that of Fe in dilute HNO₃ and H₂SO₄ acid solutions for which the increase of the potential increase the anodic current density. In the concentration range between 8 and 10M, the effect of the cathodic reaction becomes greater. In the acid concentration, more than 10 M, the anodic curve of dissolution is completely disappeared and in the reverse direction only a negative current is observed which corresponds to the cathodic reaction. In the previous work the corrosion behavior of nickel, nickel alloys and stainless steel, in acidic solutions and its inhibition was explained [11-15].

The aim of the present manuscript is to study the cyclic voltammetry curves of nickel, Inconel 600, Incoloy800 and 316 stainless in HNO₃ acid as a function of the acid concentration. All the anodic and the cathodic peaks are interpreted. The nature of the passive film formed is explained.

2. Experimental details

The chemical composition of nickel (Ni) and three alloys Inconel600, Incoloy 800 and 316 stainless steel are given in Table 1. For the cyclic voltammetry technique, a cylindrical rod embedded in Araldite with an exposed surface area of 1.7cm² for Ni, 1.57 cm² for the Inconel600, 1.48cm² for the Incoloy800 and 1.44 cm² for the 316-stainless steel was used. These electrodes were fixed to Pyrex glass tubing using neutral wax.

The electrodes were abraded with different grades of emery paper (grade 400, 600, 800, 1000 and 1200) to obtain smooth surface, degreased with acetone and rinsed with twice distilled water. The experiments were carried out at 25 ± 1°C using air thermostat. Complete wetting of the surface was taken as an indication of its cleanliness. All chemicals used were of A.R. quality. All solutions were freshly prepared by distilled water. A three-compartment cell with saturated calomel reference electrode (SCE) and a Pt foil was used as an auxiliary electrode. The potential was measured against a reference saturated calomel electrode (SCE).

Cyclic voltammetry measurements were carried out using a Wenkingpotentiostan, Type POS-73. The current density-potential curves were recorded on X-Y recorder, Type PL-3. Before carrying out any experiment, the working electrode was precathodized (for 20 minutes) at a potential of -1.5V in order to reduce the pre-immersion oxide film formed at the surface of the electrode.

Table 1. The chemical composition of the alloys used.

Alloy	Ni%	Fe%	Cr%	Cu%	Si%	P%	S%	Mn%	C%	Others%
Nickel	100	-	-	-	-	-	-	-	-	-
Inconel 600	73.42	9.33	16.10	0.03	0.118	0.007	0.006	0.38	0.04	Al 0.28, Ti 0.24, Co 0.049
Incoloy 800	33.49	44.95	19.32	0.27	0.32	-	0.007	0.81	0.063	Al 0.39, Ti 0.38
316 Stainless Steel	13.12	65.80	16.50	-	0.50	0.03	0.002	1.63	0.028	Mo 2.35

3. Results and Discussion

3.1 Effect of nitric acid concentration on the cyclic voltammetry of nickel alloys and stainless steel

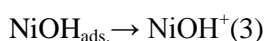
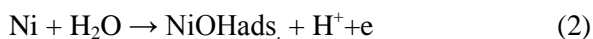
The curves of Figs.1-4 show the cyclic voltammetry (CVS) curves of nickel, Inconel600, Incoloy 800 and 316 stainless steel respectively, in varying concentrations of HNO₃ acid solutions. The potential was swept between -2V and +2V, for Ni, - 1V and + 1.5 V for the Inconel 600 and 316 stainless steel, - 1V and + 2V for Incoloy 800 at a scanning rate of 25 mV/sec.

The anodic polarization curves of Figs. (1-4) are typical of active – passive metals. All the curves are characterized by an anodic dissolution peak (A) followed by a passive region (B), before oxygen evolution. On the other hand, Incoloy 800 and 316 stainless steel (Figs. 3 and 4) show an additional dissolution peak (C) and trans passive region followed by oxygen evolution.

A characteristic feature of Ni electrode was observed during the anodic polarization curves (Fig. 1). When the electrode potential was changed towards the positive direction, an initially cathodic current was observed along a well-defined current arrest before it reaches the zero current potential values. This cathodic current is due to the evolution of hydrogen gas, according to the following reaction:



It is of interest to note, also, that the peak potential (E_p) for peak (A) Fig. 1. is more or less independent of HNO₃ concentration. This behavior confirms the irreversibility of the Ni electrode process under the present experimental conditions. Peak (A) in Figs. 1 and 2 for Ni and Inconel600 (of high Ni content) appears nearly at the same potentials indicating that, this peak may correspond to the active dissolution of Ni giving Ni²⁺ ion according to the following mechanism.



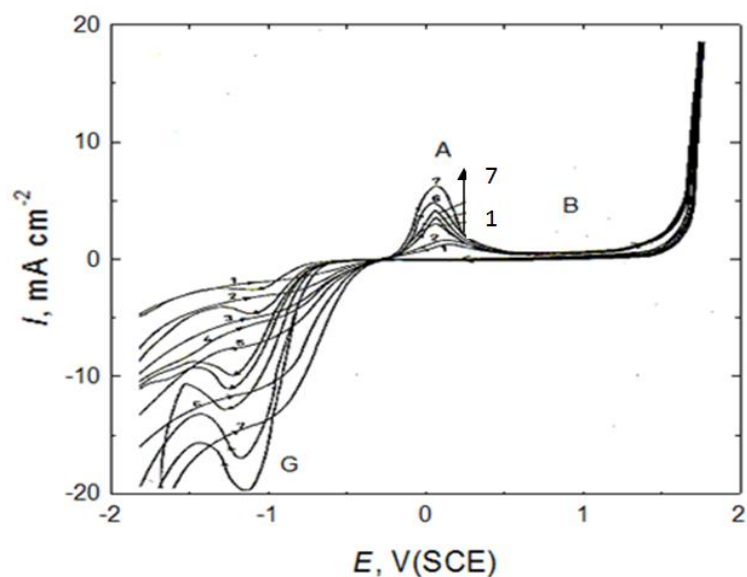


Fig.1. Cyclic voltammetry of nickel in varying concentrations of HNO₃ solution at a scan rate 25 mV/sec. 1) 0.01M HNO₃; 2) 0.03M; 3)0.05M; 4) 0.07 M; 5)0.09 M; 6)0.1 M and 7) 0.15M

Surface analysis of the passive films formed on Ni suggested that [16] the main constituents of the film in the active region is close to Ni(OH)₂. The passivation of Ni seems to occur as a result of the dehydration of nickel hydroxide film. The formation of NiO is in agreement with the results obtained from the study of the surface film formed on the Ni electrode by Raman spectroscopy [17].

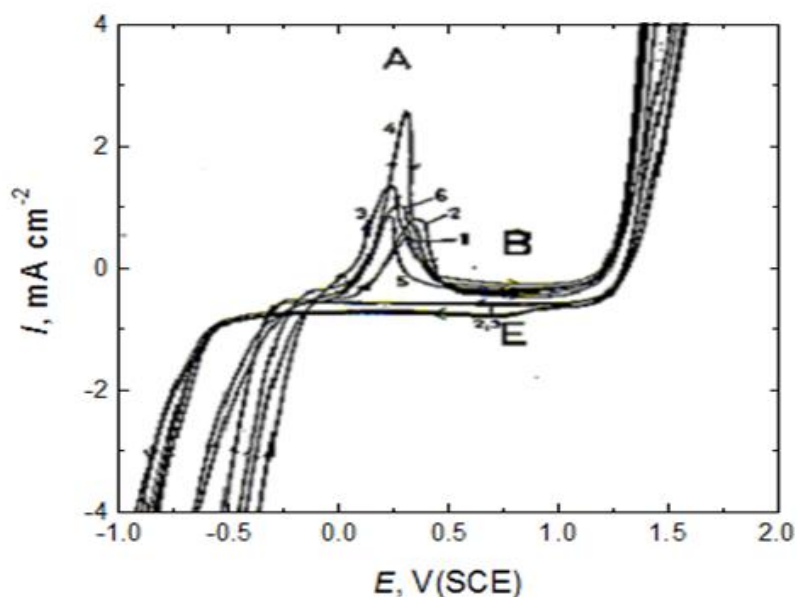


Fig. 2. Cyclic voltammetry of Inconel600 in varying concentrations of HNO₃ solution at a scan rate 25 mV/sec. 1) 0.05M HNO₃; 2) 0.07 M; 3) 1.0M; 4) 0.15 M; 5) 0.2 M and 6) 0.25 M

However, it is generally agreed that, the passive film formed on nickel in acid solutions is oxide in nature. Analysis of the composition of this film by electron diffraction, ellipsometry and electrochemical measurements assigned that it is NiO[18,19], Ni₃O₄ or duplex oxide of NiO and Ni₃O₄[20], depending upon the experimental conditions.

Further inspection of Figs. (1 and 2) for Ni and Inconel 600 reveals that a decrease of the active dissolution anodic current density of Inconel 600 than that for Ni. This is attributed to the presence of Cr in the alloy. However, Bond and Uhlig [21] reported that the critical current density of Ni-Cr alloys decreased rather sharply with the increase of chromium content, and reached a constant value at approximately 15% chromium. On the other hand, Trabanelli et al., [22] observed that, the passivity of Inconel 600 was superior to that of Ni in acidic solutions. They attributed this quality to the presence of chromium. An additional support to this hypothesis is

the XPS study of the passive film formed on a nickel and the Inconel600 in acid solutions [23]. The results showed the presence of Cr^{3+} in addition to Ni^{2+} in the passive film of the alloy

Comparison of Figs.3 and 4 for Incoloy 800 and 316 stainless steel, respectively, show qualitatively similar features in the CVS curves. If these curves are compared quantitatively, it can be seen that, the dissolution rate of Incoloy 800 (Ni content 33.44%) is much faster than 316 stainless steel (Ni content 13.72%). But it was reported before that, addition of nickel to iron – chromium alloys increase their corrosion resistance[21,22].

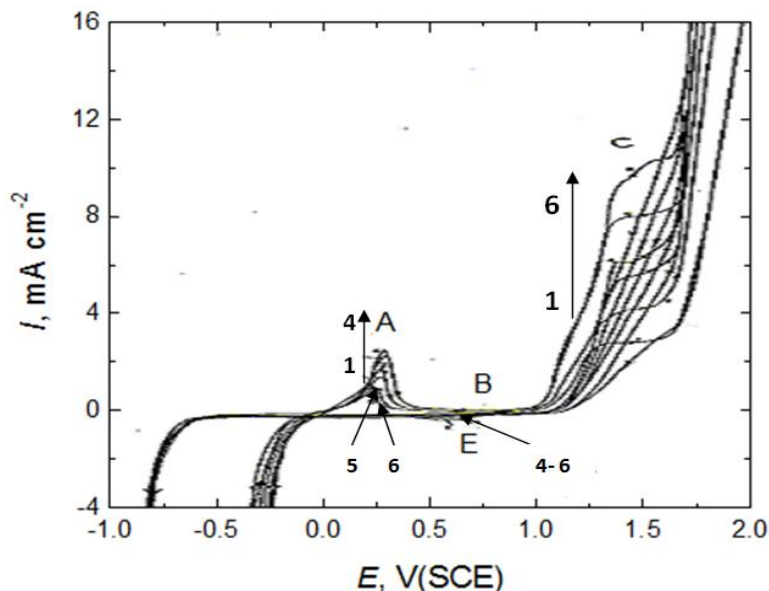


Fig. 3. Cyclic voltammetry of Incoloy 800 in varying concentrations of HNO_3 solution at a scan rate 25 mV/sec. 1) 1.0M HNO_3 ; 2) 0.15 M ; 3) 0.2 M ; 4) 0.25 M ; 5) 0.3 M and 6) 0.35 M

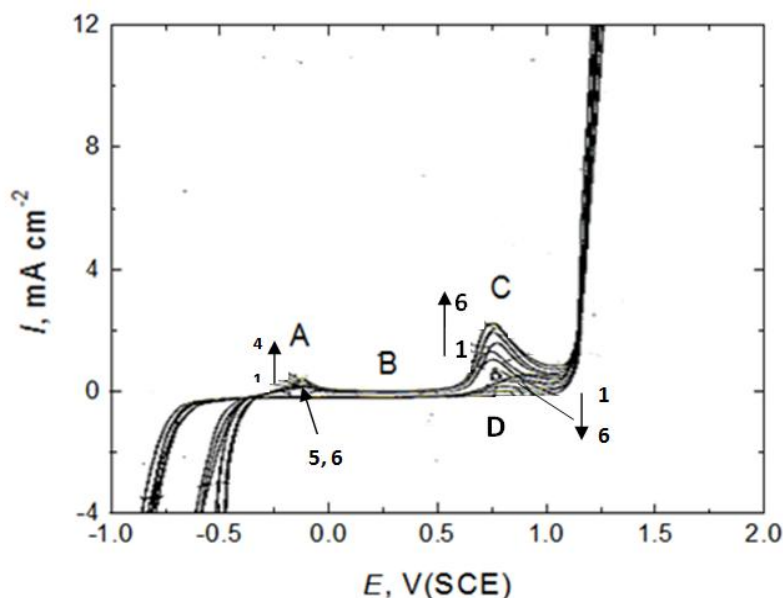


Fig. 4. Cyclic voltammetry of Incoloy800 in varying concentrations of HNO_3 solution at a scan rate 25mV/sec.1) 1.0M HNO_3 ; 2) 0.15 M ; 3) 0.2 M ; 4) 0.25 M ; 5) 0.3 M and 6) 0.35 M

Therefore, one can attribute the reverse order obtained for the inclusion of Mo in 316 stainless steel. However, according to XPS study of the passive films formed on Cr-Ni steels containing Mo, showed that it consists, mainly, of Cr^{3+} , Fe^{3+} , Ni^{2+} and Mo^{6+} [24]. The Mo ion appears in the passive film as Mo^{4+} and Mo^{6+} and was identified as hydrated MoO_2 and MO_4^{2-} . Themolybdate anions (MO_4^{2-}) are formed in the solid state along with CrO_4^{2-} . These together are responsible for producing a bipolar film containing CrO_4^{2-} and MO_4^{2-} . Among these ions Cr^{3+} and Mo^{6+} should play a very important role in improving the corrosion resistance of the film. The

corrosion resistance of steels should increase when films which are mainly composed of Cr³⁺ and Mo⁶⁺ oxides are formed on the surface of the steels. This interpretation is made in view of the fact that Mo⁶⁺ oxide (e.g. Mo₂O₃) cannot form by itself a compact surface film having a good resistance to corrosion. Pure Mo dissolves with a large rate producing an unprotected oxide film of Mo₂O₃ in the potential range above ±0.0V [24]. On the other hand, the observed phenomenon that the current density in the passive state of Fe-Mo binary alloys increases with increase in Mo content, supports the above interpretation

Peak (C), which appears in the case of Incoloy 800 and 316 stainless steel, as shown in Figs. (3 and 4), respectively, can be ascribed to the electro-oxidation of Cr (III), which present in the passive film to Cr (VI). This assumption is based on the results reported by other workers [25]. The potential of peak (C) is close to the equilibrium potential of the reaction.



This implies that, the protective Cr (III) species formed in the passive film are electro oxidized to soluble Cr (VI). This behavior was further illustrated by the work carried on a high purity Fe - 9 Cr - 8 Ni alloy[26]. Photoelectron spectra showed that, at high potentials CrO₄²⁻ is formed at the metal – electrolyte interface, and is lost from the surface by dissolution.

Electro oxidation of Cr (III) to soluble Cr (VI) implies the simultaneous replacement of Cr (III) by iron in the passive layer. Augar spectroscopy of the passive films formed on 316 stainless steel supported this fact. The data showed a decrease in the Cr / Fe ratio in the passive film as the potential moves from 0.0V to the oxygen evolution threshold potential [25].

In order to throw more light, on the anodic oxidation peak (C) which observed in the CVS of Incoloy 800 and 316stainless steel (Figs.3 and 4), the influence of the presence of chromium ions in solution is studied by anodic polarization of pure iron electrode in 0.1 M nitric acid (curve 1) and 0.1 M nitric acid + 0.2M K₂CrO₄ (curve 2) in Fig. (5) at 25 mVS⁻¹. Radioactive tracing studies of film growth on steel in inhibitive solutions using potassium chromate labeled with ³¹Cr showed that only trace of Cr (VI) was detected in the surface film. It was assumed that, Cr is, thus, deposited as Cr (III), that is Cr₂O₃ [26]. Therefore, the properties of the passive film are reproduced, i.e. inclusion of Cr (III) in the passive film on the iron electrode surface. Thus, the appearance of peak (C) at high potentials (Curve 2 Fig. 5) confirms the above postulation that, it is attributed to the electro-oxidation of Cr (III) to Cr (IV).

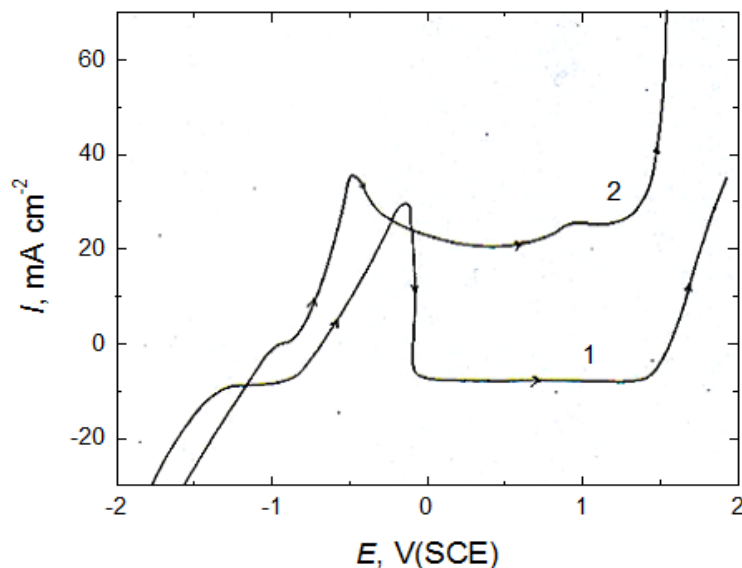


Fig. 5. Anodic polarization curves recorded at a scan rate 25mV/sec. for: 1) Fe in 0.1M HNO₃ ;2) Fe in 0.1M HNO₃+ 0.2 M K₂CrO₄

Inspection of Fig. 2 for the Inconel 600 reveal that, peak C does not appear and the current increases rapidly about the potential at which electro-oxidation of Cr (III) to Cr (VI) occurs. It is quite evident that Inconel 600 does not exhibit a secondary passivity, but corrodes at an increasing rate with increasing the potential.

When the potential of the working electrode is reversed in the cathodic direction after oxygen evolution, there is one cathodic peak (G) appears, only, in case of Ni as shown in Fig. (1). Therefore, the cyclic voltammetry of nickel in 0.1M HNO₃ was performed at a scanning rate of 25 mV s⁻¹ between the potentials of -1.5V and -0.2V (i.e. before peak A). The curve obtained in Fig. 6 showed that, there is only one cathodic peak (peak G). This illustrates that this peak (G) does not correspond to the reduction of the anodic peak (A) but corresponds to the hydrogen evolution. This behavior indicates, again, that the dissolution and passivation of nickel electrode in HNO₃ solution is an irreversible process.

Inspection of the curves of Figs. (3 and 4) for the Incoloy 800 and 316 stainless steel, respectively, show that, a new cathodic peak (E) appears on the cathodic branch of the CVS at 0.5V. This peak was found to be dependent upon the acid concentration. The appearance of peak (E) can be attributed to the reduction of some materials formed in the anodic region, i.e. reduction of Cr (VI) to Cr (III). The fact that the reduction peak (E) is associated with the Cr (VI) to Cr (III) transition was confirmed by a separated experiment. The alloys were passivated at potentials > 1V and before oxygen evolution in a cell containing 0.1 M HNO₃ acid. Then washed under running water and transferred to another cell containing a fresh quantity of HNO₃ acid. On cathodic reduction, the alloys still produced the same type of CVS showing the reduction peak (E) Fig.6, Therefore, one can safely conclude that, the reduction peak (E) is not likely to be due to the reduction of Cr (VI) species in solution.

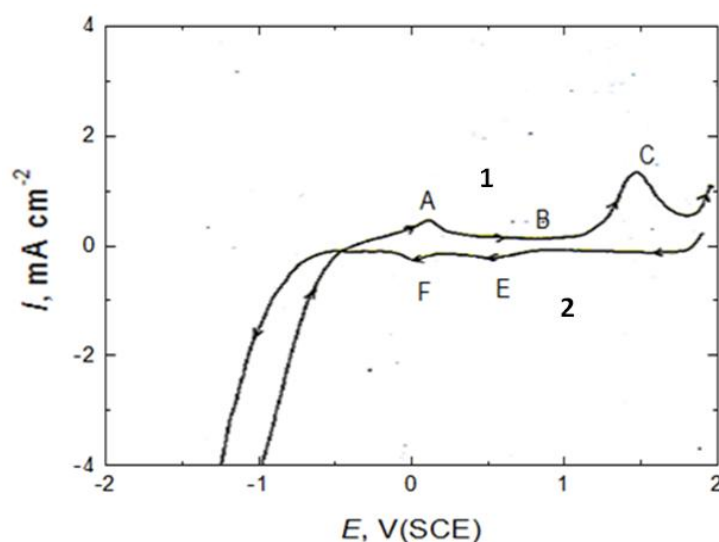


Fig.6. Curve (1) represents the anodic polarization of Incoloy 800 in 0.1M HNO₃ (at 100 mV/sec).

Curve (2) represents the cathodic reduction of the materials formed during the anodic polarization after washing the electrode under running water, in fresh 0.1 M HNO₃ solution (at 100 mV/sec).

On the other hand, the curves of 316 stainless steel, Fig.4, show that, when the potential of the working electrode is reversed in the cathodic direction after oxygen evolution, current drops. Then an unexpected peak (D) is observed in the anodic branch of the CVS. This peak is mostly due to a continuous dissolution of the electrode at a rate as that of the anodic dissolution along the active region [27]. However, Sato et al. [28] found that, the amount of reductively dissolved iron during cathodic reduction of the anodic oxide film formed on iron in boric –borate solutions, exceeds the amount calculated from the charge of the anodic oxide film assuming iron (III) is formed. He attributed this phenomenon to the dissolution of the underlying iron, which would occur at a higher rate in acid solutions.

Fig 7(a and b) represents the relation between the dissolution current density (I_{peak}) and the molar concentrations of HNO₃ solution on a double logarithmic scale for peaks A and C, respectively. In case of peak "A", the results of Ni satisfy a straight-line relationship according to the following equation:

$$\text{Log } I_{peak} = a + b \text{ log } C_{HNO_3} \quad (6)$$

where, a and b are constants depending upon the scanning rate and the type of the electrode. For the other alloys, the relationship satisfies equation (6) up to a concentration of 0.15M, 0.25M and 0.25M for Inconel600, Incoloy 800 and 316 stainless steel.

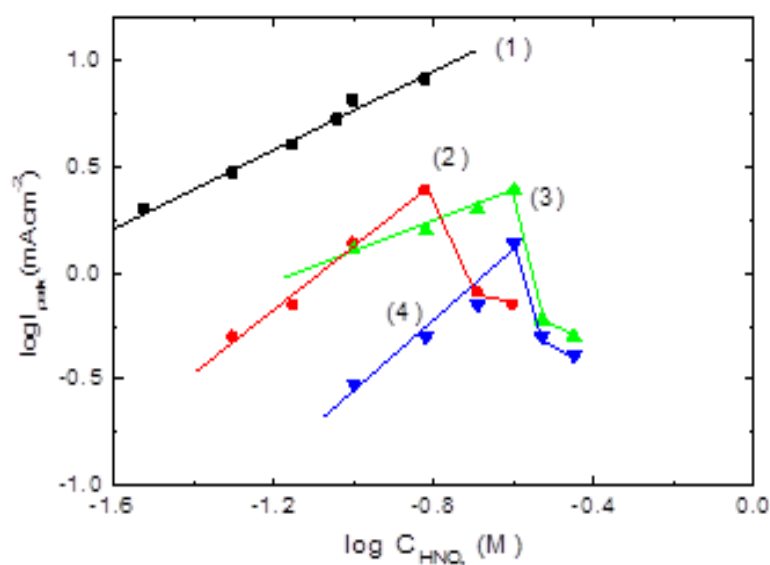


Fig. 7a. The relation between the dissolution current density for peak (A) versus the molar concentration of HNO_3 solution on a double logarithmic scale. 1-Ni ; 2-Inconel600; 3-Incoloy 800 ; 4-316 stainless steel

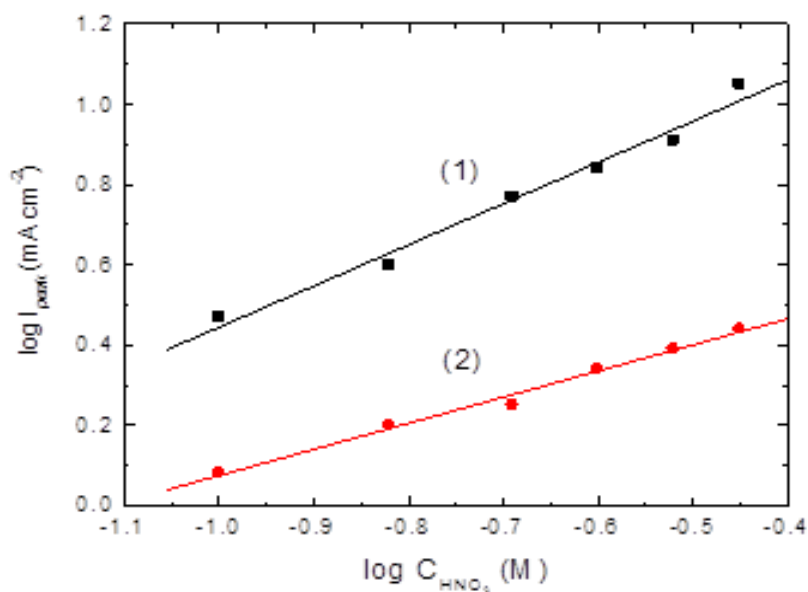


Fig. 7 b. The relation between the dissolution current density for peak (C) versus the molar concentrations of HNO_3 solution on a double logarithmic scale: 1- Incoloy 800 and 2- 316 stainless steel

This indicates that, the rate of dissolution of Ni and three alloys increase with the increase of HNO_3 acid concentration. At concentrations higher than the above-mentioned ones, the relationship is reversed in the opposite direction, i.e. the sign between the two terms of the equation (6) becomes negative]. This behavior may be attributed to the oxidizing properties of HNO_3 acid at high concentrations. Under such conditions, the passivation of the electrode is enhanced and consequently its rate of dissolution is decreased.

In case of peak (C) which appears only for Incoloy 800 and 316 stainless steel, straight-line relationship satisfies equation (6) at all concentrations. Thus, one can assume that, the rate of electro oxidation of Cr (III) to Cr (VI) increases as the concentration of the oxidizing HNO_3 acid is increased.

Conclusion

1. Cyclic voltammetry were constructed for nickel, Inconel600, Incoloy800 and 316 stainless steel in various concentrations of HNO₃.
2. All the curves in the anodic branch are characterized by peak (A) followed by a passive region (B), an additional peak (C) and trans passive region followed by oxygen evolution are observed in incoloy800and 316 stainless steel
3. The main constituent of the passive film in Ni is NiO.
4. The passive film in the alloys consists of Ni⁺², Fe⁺³ and Cr⁺³ oxides in addition to the Mo⁺⁶oxide in case of 316 stainless steel.
5. In the cathodic branch of the CVS there is one cathodic peak in the case of Ni. Inconel600 and Incoloy800. On the other hand, there is an unexpected peak in case of 316 stainless steel. This peak appeared on the anodic branch.

References

1. Elewady, G. Y., El-Askalany, A. H., M. F., *Port. Electrochim Acta* 26 (2008) 503.
2. Hamed, E., Abed El-Rehim S. S., El-Shaht M. F., Shaltot A. M., *Mater. Sci. Eng.B* 177 (2012) 441.
3. Kear G., Barker B. D., Stocker K. R., Walsh F. C., *J. Appl. Electrochem.* 34 (2004) 1235.
4. Abd El Aal E.E., Zakaria W., Diab A., Abd.El-Haleem S.M., *Anti Corros. Methods Mater.* 48 (2001) 181.
5. Abed El Haleem S. M., Abd El Wanees S., *Mater. Chem. Phys.* 128 (2011) 418.
6. Munoz A.I., Anton J. G., legion J., Herranz V. P., *Corros. Sci.* 48 (2006) 3349.
7. Zheng S.Q., Wang D.N., Qi Y.M., Chen C.F., Chen L.Q., *Int. J. Electrochem. Sci.* 7 (2012) 12974.
8. Abdallah M., Abd El-Haleem S. M., *Bull. Electrochem.* 12 (1996) 449.
9. Abdallah M., Megahed H. E., El-Naggar M., Radwan D., Mabrouk E. M., *Bull. Electrochem.* 19 (2003) 245.
10. Stunick-lisac E., Karsulin M., *Electrochem. Acta* 29 (1984) 1339.
11. Abdallah M., El-Etre A. Y., *Port. Electrochim. Acta*, 21 (2003) 315.
12. Fouda A.S., Farahat M. M., Abdallah M., *Res. Chem. Intermed.* 40 (2014) 1249.
13. Abdallah M., Al Karane S. A., Abdel Fattah A.A., *Chem. Engineering Comm.* 197 (2010) 1446.
14. Mabrouk E.M., Megahed H. E., Abdallah M., Abdel Fattah A.A., *Bull. Electrochem.* 11 (1995) 217.
15. Abdallah M., El-Naggar M., Megahed H. E., Radwan D., Mabrouk E. M., *Corros. Preven. Cont.* 50 (2003) 173.
16. Sugamoto K., Sawada Y., *Chorus. Sci.* 17 (1977) 425.
17. Pierre D., Augot A., Le Gove, Nig Yu, *J. Electrochem. Soc.* 133 (1986) 2106.
18. Khaled K.F., *Electrochim. Acta* 55 (2010) 5375.
19. Mary H. W., Rebecca J. L. Zorbakhsh W. A., Gutfreund P., Clarke S. M., *Langmuir* 31 (2015) 7062.
20. Cowan R.L., Staehle R. W., *J. Electrochem. Soc.* 118 (1971) 557.
21. Bond A. P., Uhlig H. H., *J. Electrochem. Soc.* 107 (1960) 488.
22. Trabaneli G., Zucchi F., Felloni L., *Corros. Sci.* 5 (1965) 211.
23. Kawashima A., Asami K., Hashimoto K., *Corros. Sci.* 25 (1985) 1103.
24. Sugamoto K., Sawada Y., *Corros. Sci.* 17 (1977) 425.
25. Ramasubramanian N., Preocanin N., Davidson R. D., *J. Electrochem. Soc.* 132 (1985) 793.
26. Brooks A. R., Clayton C. R., Doss K, Lu Y. C., *J. Electrochem. Soc.* 133 (1986) 2459.
27. Abdallah M., Megahed H. E., *Monatsh fur Chemie*; 126 (1995) 519.
28. Sato N, Kudo K., Noda T., *Electrochim. Acta* 16 (1971) 1909.

(2017) ; <http://www.jmaterenvirosci.com>